**Supplementary Table 1.** Uncertainties of $\Delta C_{ant}$ induced changes in each acidification metric ($\Delta pCO_{2u}$, $\Delta H_u$, $\Delta pH_u$, $\Delta\Omega_u$ and $\Delta RF_u$) in the upper 50m (0~50m), the upper and lower OMZs ($OMZ_u$ and $OMZ_l$) and the comparable well-ventilated area in the south ($Vent_u$ and $Vent_l$). Also, presented are the corresponding uncertainties in the North Atlantic well-ventilated waters ($Vent_{Nu}$ and $Vent_{Nl}$).

| | | $\Delta pCO_{2u}$ (μatm) | $\Delta H_u$ (nmol kg$^{-1}$) | $\Delta pH_u$ | $\Delta\Omega_u$ | $\Delta RF_u$ |
|---|---|---|---|---|---|---|
| P16 | 0~50m | 28±8 | 0.57±0.17 | 0.03±0.01 | 0.21±0.07 | 0.3±0.1 |
| | $OMZ_u$ | 129±31 | 2.76±0.68 | 0.06±0.01 | 0.10±0.03 | 0.4±0.2 |
| | $OMZ_l$ | 129±27 | 3.00±0.60 | 0.06±0.01 | 0.08±0.02 | 0.3±0.2 |
| | $Vent_u$ | 37±8 | 0.81±0.20 | 0.04±0.01 | 0.16±0.03 | 0.6±0.1 |
| | $Vent_l$ | 64±15 | 1.57±0.40 | 0.05±0.01 | 0.11±0.02 | 0.8±0.2 |
| I9N&S | 0~50m | 33±12 | 0.64±0.25 | 0.04±0.01 | 0.26±0.11 | 0.3±0.1 |
| | $OMZ_u$ | 94±39 | 1.91±0.81 | 0.05±0.01 | 0.14±0.04 | 0.6±0.1 |
| | $OMZ_l$ | 102±30 | 2.27±0.65 | 0.06±0.01 | 0.11±0.02 | 0.6±0.1 |
| | $Vent_u$ | 47±21 | 1.00±0.46 | 0.05±0.02 | 0.25±0.10 | 0.7±0.4 |
| | $Vent_l$ | 80±36 | 1.89±0.87 | 0.07±0.03 | 0.18±0.07 | 1.1±0.5 |
| A16 | 0~50m | 30±15 | 0.58±0.28 | 0.03±0.02 | 0.26±0.14 | 0.3±0.1 |
| | $OMZ_u$ | 83±20 | 1.73±0.44 | 0.05±0.01 | 0.13±0.03 | 0.7±0.2 |
| | $OMZ_l$ | 97±18 | 2.10±0.38 | 0.05±0.01 | 0.12±0.03 | 0.7±0.2 |
| | $Vent_u$ | 41±16 | 0.90±0.35 | 0.05±0.02 | 0.19±0.06 | 0.6±0.3 |
| | $Vent_l$ | 52±16 | 1.18±0.37 | 0.05±0.01 | 0.15±0.03 | 0.8±0.2 |
| | $Vent_{Nu}$ | 27±5 | 0.57±0.11 | 0.03±0.00 | 0.15±0.02 | 0.4±0.1 |
| | $Vent_{Nl}$ | 37±6 | 0.80±0.13 | 0.04±0.01 | 0.13±0.02 | 0.5±0.1 |

**Supplementary Table 2.** Changes of each acidification metric to unit $\Delta C_{ant}$ within the poorly versus well-ventilated waters. Here the mean water age, preindustrial RF (RF_PI), changes of each acidification metric due to unit $\Delta C_{ant}$ ($\Omega_{uc}$, $pH_{uc}$, $H_{uc}$ and $pCO_{2uc}$) in the upper 50m (0~50m), the upper and lower OMZs ($OMZ_u$ and $OMZ_l$) and the comparable well-ventilated area in the south ($Vent_u$ and $Vent_l$). Also, presented are the corresponding changes in the North Atlantic well-ventilated waters ($Vent_{Nu}$ and $Vent_{Nl}$).

| | | Water age (year) | RF-PI | $1000pH_{uc}$ (units/μmol kg$^{-1}$) | $1000\Omega_{uc}$ (units/μmol kg$^{-1}$) | $H_{uc}$ (nmol kg$^{-1}$/μmol kg$^{-1}$) | $pCO_{2uc}$ (μatm/μmol kg$^{-1}$) |
|---|---|---|---|---|---|---|---|
| P16 | 0~50m | 2±2 | 9.2±1.3 | -1.7±0.3 | -9.9±0.5 | 0.03±0.01 | 1.6±0.3 |
| | $OMZ_u$ | 163±77 | 17.6±1.6 | -3.2±0.2 | -5.6±1.3 | 0.16±0.04 | 7.7±1.7 |
| | $OMZ_l$ | 677±168 | 18.8±0.4 | -3.2±0.1 | -4.3±0.7 | 0.17±0.02 | 7.7±1.1 |
| | $Vent_u$ | 22±24 | 12.1±1.2 | -2.3±0.2 | -8.3±0.6 | 0.05±0.01 | 2.3±0.4 |
| | $Vent_l$ | 302±216 | 16.0±1.1 | -2.9±0.1 | -5.8±0.8 | 0.09±0.01 | 3.8±0.5 |
| I9N8S | 0~50m | 4±3 | 8.2±0.2 | -1.6±0.0 | -10.3±0.1 | 0.03±0.00 | 1.5±0.1 |
| | $OMZ_u$ | 124±78 | 15.0±1.8 | -2.7±0.3 | -7.5±0.9 | 0.11±0.03 | 5.6±1.3 |
| | $OMZ_l$ | 556±126 | 17.7±0.3 | -3.1±0.1 | -5.5±0.3 | 0.14±0.01 | 6.3±0.8 |
| | $Vent_u$ | 15±11 | 11.3±1.1 | -2.1±0.2 | -8.7±0.5 | 0.04±0.01 | 2.0±0.4 |
| | $Vent_l$ | 176±133 | 15.1±1.6 | -2.8±0.2 | -6.5±0.9 | 0.08±0.02 | 3.4±0.6 |
| A16 | 0~50m | 1±0 | 8.3±0.3 | -1.4±0.0 | -10.1±0.1 | 0.03±0.00 | 1.5±0.0 |
| | $OMZ_u$ | 128±79 | 15.3±1.3 | -2.8±0.2 | -7.2±0.7 | 0.10±0.02 | 5.1±0.7 |
| | $OMZ_l$ | 375±38 | 17.3±0.2 | -3.2±0.1 | -6.1±0.1 | 0.13±0.01 | 6.3±0.3 |
| | $Vent_u$ | 17±19 | 11.8±1.7 | -2.2±0.3 | -8.5±0.7 | 0.04±0.01 | 2.1±0.5 |
| | $Vent_l$ | 49±37 | 14.1±1.0 | -2.7±0.2 | -7.3±0.3 | 0.06±0.01 | 2.9±0.4 |
| | $Vent_{Nu}$ | 8±6 | 10.5±0.8 | -1.9±0.2 | -8.9±0.4 | 0.04±0.01 | 1.8±0.3 |
| | $Vent_{Nl}$ | 29±11 | 12.0±0.3 | -2.2±0.0 | -7.9±0.1 | 0.05±0.00 | 2.4±0.1 |

**Supplementary Table 3.** Water properties and changes in $CO_2$ species and $[H^+]$ induced by 1 μmol $kg^{-1}$ addition of DIC. Parameters are presented for the upper 50m (0-50m) and the upper OMZ ($OMZ_u$) along section P16. Properties include water depth, salinity, temperature, TA, DIC, $[CO_3^{2-}]$, and borate ion concentration ($[B(OH)_4^-]$), along with related RF values. Also shown are changes in $CO_2$ species, including $pCO_{2uc}$, $H_{uc}$, $pH_{uc}$, and $\Omega_{uc}$. Additionally, the table lists the concentrations of undissociated $CO_2^*$ in seawater, produced $H^+$ from $CO_2^*$ dissociation, consumed $H^+$ by carbonate, borate, hydroxide, and other minor species, residual $H^+$ after consumption, and the percentage of residual $[H^+]$ relative to the initial $[H^+]$ produced (Residual H%) as well as consumed $CO_3^{2-}$ by $H^+$. Note that the concentrations of undissociated $CO_2^*$ in seawater and residual $[H^+]$ after consumption determine the changes of seawater $pCO_2$ and pH after the addition of DIC.

| | 0~ 50m | $OMZ_u$ |
|---|---|---|
| Depth (m) | 22 | 421 |
| Salinity | 34.41 | 34.37 |
| Temperature (°C) | 20.78 | 7.29 |
| TA (μmol $kg^{-1}$) | 2277 | 2312 |
| DIC (μmol $kg^{-1}$) | 1939 | 2257 |
| $[CO_3^{2-}]$ (μmol $kg^{-1}$) | 233 | 61 |
| $[B(OH)_4^-]$ (μmol $kg^{-1}$) | 107 | 32 |
| RF | 9 | 18 |
| $pCO_{2uc}$ (μatm) | 1 | 7 |
| $H_{uc}$ (nmol $kg^{-1}$) | 0.025 | 0.146 |
| $pH_{uc}$ | -0.0016 | -0.0032 |
| $\Omega_{uc}$ | -0.015 | -0.009 |
| Undissociated $CO_2^*$ (μmol $kg^{-1}$) | 0.04 | 0.34 |
| Produced $H^+$ by $CO_2^*$ dissociation (nmol $kg^{-1}$) | 959.405 | 657.734 |
| Consumed $H^+$ (nmol $kg^{-1}$) | 959.380 | 657.584 |
| Residual $H^+$ (nmol $kg^{-1}$) | 0.025 | 0.150 |
| Consumed $CO_3^{2-}$ (μmol $kg^{-1}$) | -0.64 | -0.43 |

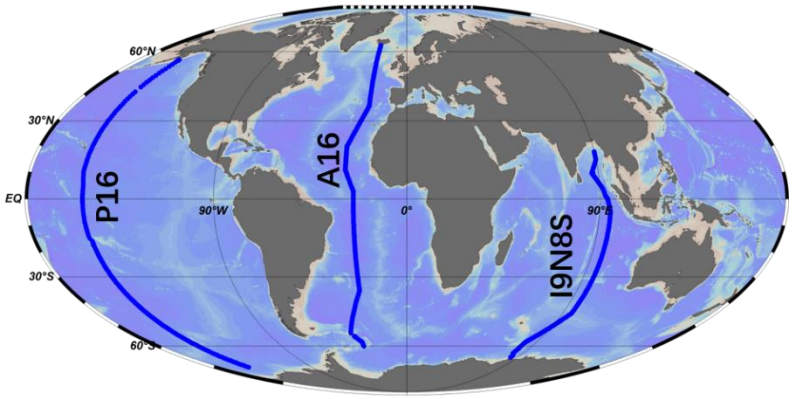


**Supplementary Fig. 1** Locations of sections P16, I9N8S, and A16 in the global ocean.

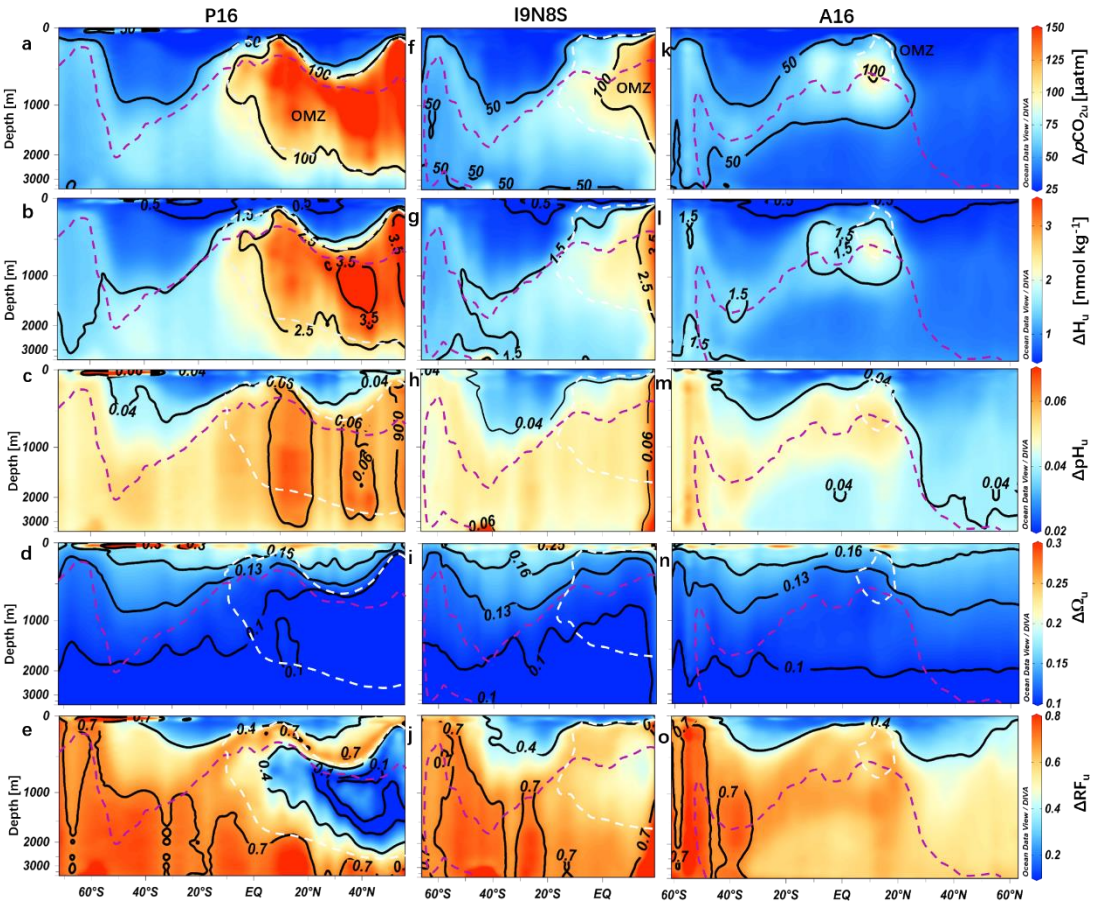


**Supplementary Fig. 2** Uncertainties of $\Delta C_{ant}$ induced changes in each acidification metric. Panels (a) - (e) display the vertical distributions of uncertainties in $\Delta pCO_2$ ($\Delta pCO_{2u}$, a), $\Delta[H^+]$ ($\Delta H_u$, b), $\Delta pH$ ($\Delta pH_u$, c), $\Delta\Omega_{ara}$ ($\Delta\Omega_u$, d), and $\Delta RF$ ($\Delta RF_u$, e). Panels (f) - (j) display the same parameters but along section I9N8S; Panels (k) - (o) display the same parameters but along section A16.

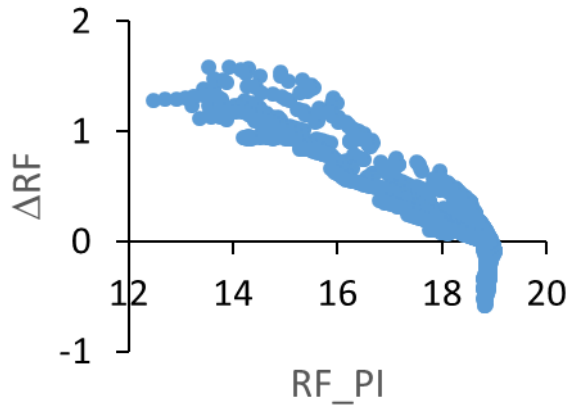


**Supplementary Fig. 3** Scatterplots of initial RF values for the preindustrial era (RF_PI) versus ΔRF within the upper OMZ of section P16.

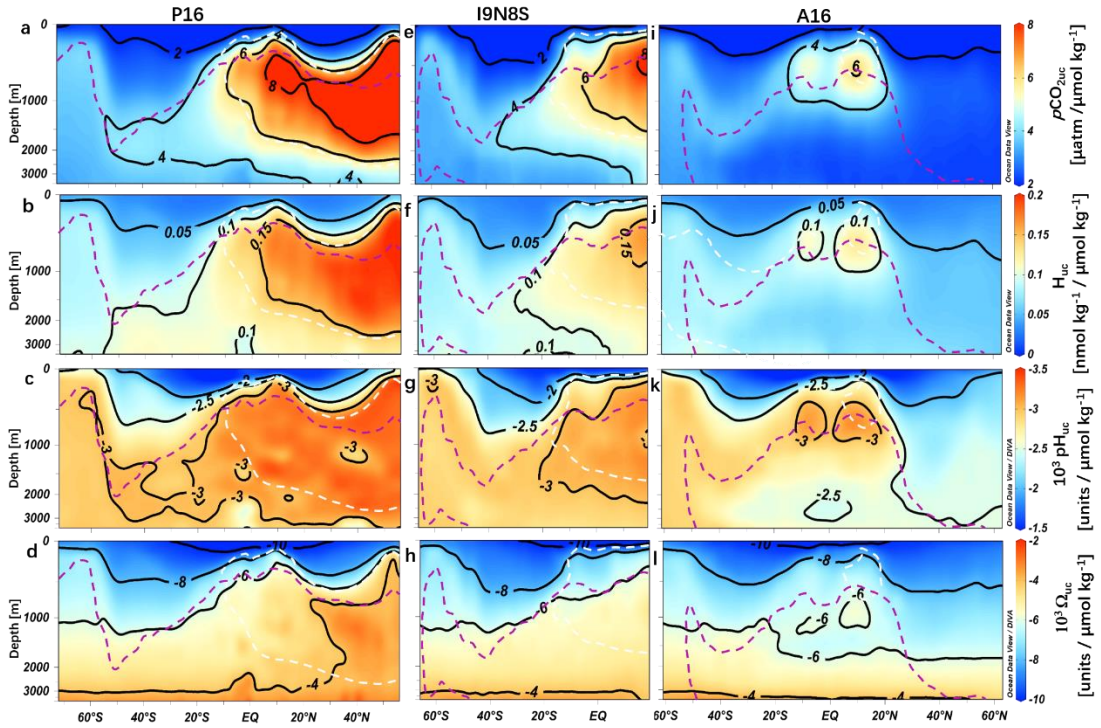


**Supplementary Fig. 4** Changes of each acidification metric due to unit $\Delta C_{ant}$. Panels (a) - (d) display the vertical distributions of unit $\Delta C_{ant}$ induced changes in $pCO_2$ ($pCO_{2uc}$, a), $[H^+]$ ($H_{uc}$, b), pH ($10^3pH_{uc}$, c) and $\Omega_{ara}$ ($10^3\Omega_{uc}$, d). Panels (e) - (h) display the same parameters but along section I9N8S; Panels (i) - (l) display the same parameters but along section A16.

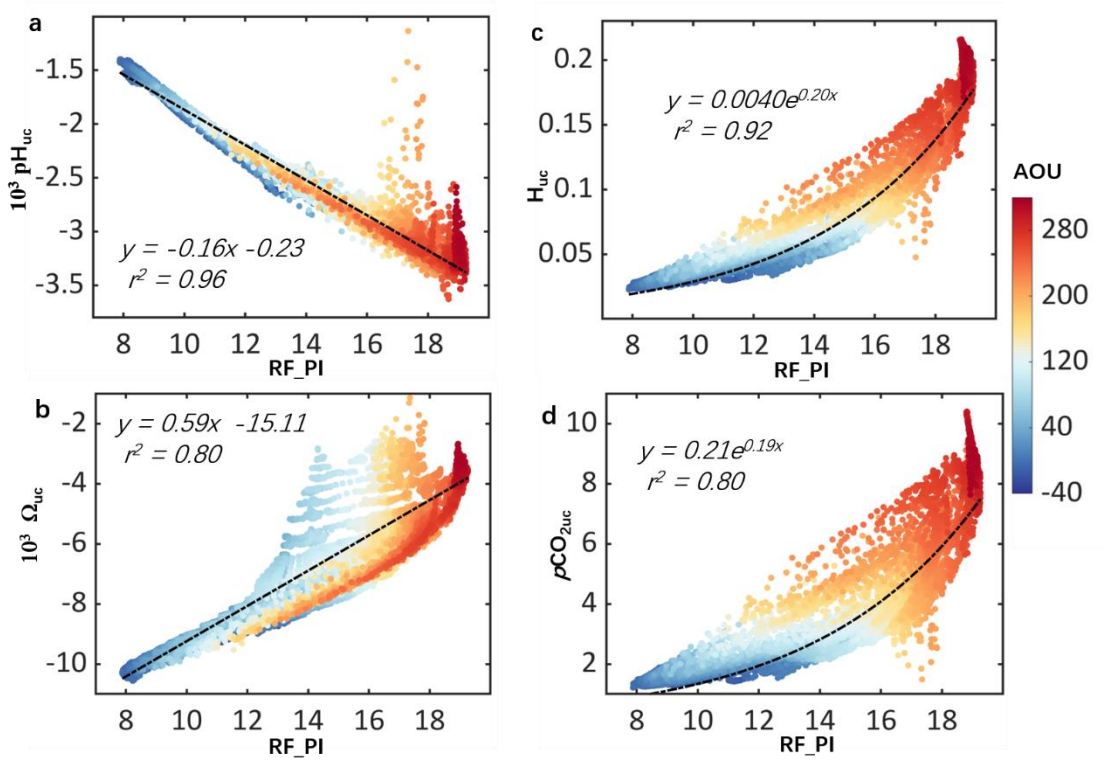


**Supplementary Fig. 5** Relationships between changes in acidification metrics due to unit $\Delta C_{ant}$ and the Revelle factor. Panels (a)-(d) show the relationships of Revelle factor during the preindustrial era (RF_PI) with unit $\Delta C_{ant}$ induced declines in pH ($pH_{uc}$, a) and $\Omega_{ara}$ ($\Omega_{uc}$, b), as well as the increases in $[H^+]$ ($H_{uc}$, c) and $pCO_2$ ($pCO_{2uc}$, d). Also, in each panel the apparent oxygen utilization (AOU) is shown with the color bar.

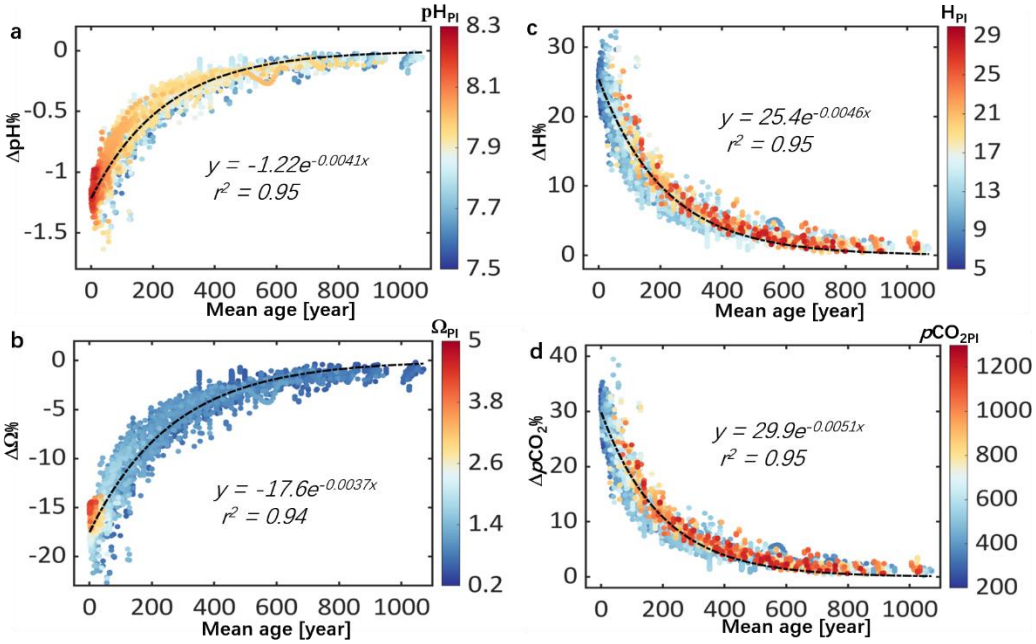


**Supplementary Fig. 6** Correlations between relative changes in acidification metrics and water age. Panels (a)-(d) show the relationships of the water age with the relative changes of pH ($\Delta pH_{\%}$, a), $\Omega_{ara}$ ($\Delta\Omega\%$, b), $[H^+]$ ($\Delta H_{\%}$, c) and $pCO_2$ ($\Delta pCO_{2\%}$, d). Also, in each panel the values of acidification metrics during the preindustrial era are shown with color bar.

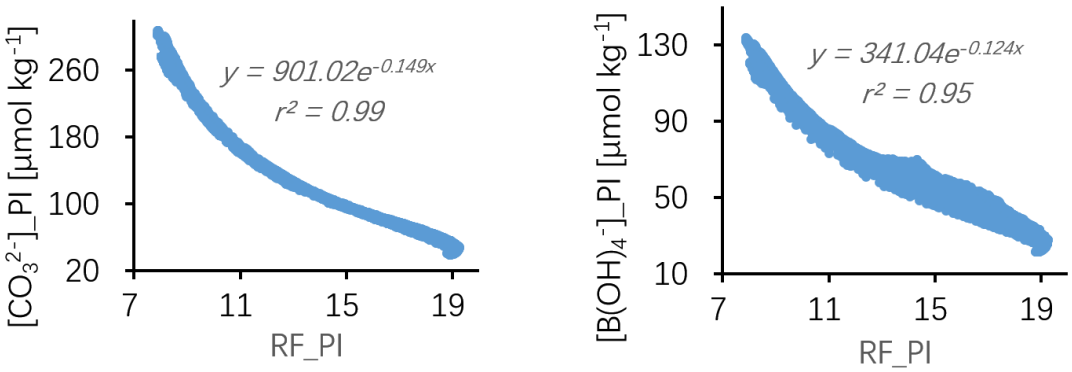


**Supplementary Fig. 7** Correlations between carbonate ions and borate ions with RF. Panels (a)-(b) show the relationships of RF values with carbonate ion concentrations ($[CO_3^{2-}]$, a) and borate ion concentrations ($[B(OH)_4^-]$, b). $[CO_3^{2-}]$_PI, $[B(OH)_4^-]$_PI and RF_PI are the $[CO_3^{2-}]$, $[B(OH)_4^-]$ and DIC during the preindustrial era.

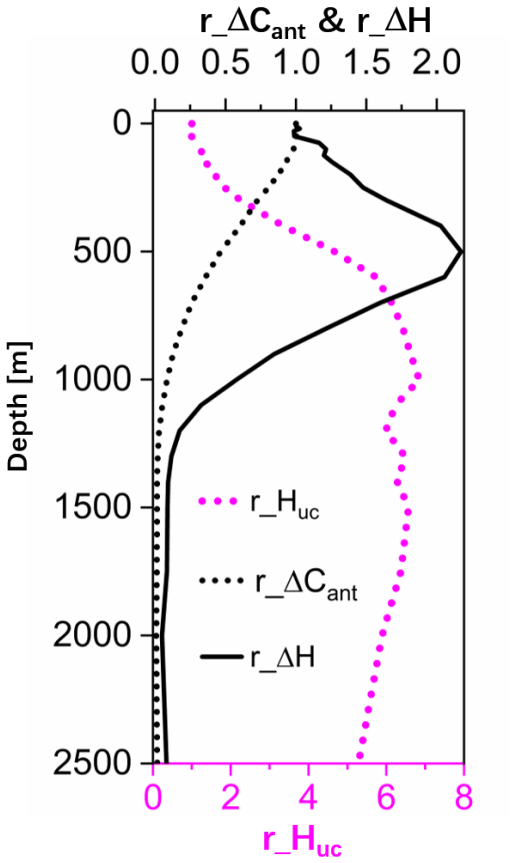


**Supplementary Fig. 8** Ratios of $H_{uc}$, $\Delta C_{ant}$ and $\Delta[H^+]$ in ocean interior relative to the surface. This figure shows the ratios of $H_{uc}$ (r_ $H_{uc}$, pink dashed line), $\Delta C_{ant}$ (r_$\Delta C_{ant}$, black dashed line) and $\Delta[H^+]$ (r_ΔH, black solid line) in ocean interior relative to the surface in a typical OMZ station located in the North Pacific (42.5°N, 152.5°W). Here we use r_ $H_{uc}$ to denote the increase in acidification by a weaker buffering capacity and r_$\Delta C_{ant}$ to denote decrease in acidification by weaker ventilation.